Carbon–Carbon Bond Formation on Multisite-Bound Unsaturated Ligands: Synthesis of μ_2-η^2-Allenyl Complexes via Carbene Addition to the Binuclear Acetylides Ru$_2$(CO)$_6$(μ_2-η^2-C≡CR)(μ-PPh$_2$)

Donato Nucciarone, Nicholas J. Taylor, and Arthur J. Carty*

Guelph-Waterloo Centre for Graduate Work in Chemistry, Waterloo Campus, Department of Chemistry, University of Waterloo, Waterloo, Ontario, Canada N2L 3G1

Reaction of Ru$_2$(CO)$_6$(μ_2-η^2-C≡CPh)(μ-PPh$_2$) with N$_2$CR$_2$ (R = H, CH$_3$, C$_6$H$_5$) results in formation of Ru$_2$(CO)$_6$(μ_2-η^2-R$_2$C=C=CPh)(μ-PPh$_2$) (3a–c) in moderate to good yields. Compounds 3a–c have been fully characterized by infrared and ^{1}H and ^{31}P NMR spectroscopy as well as elemental analyses. A complete, single-crystal, X-ray diffraction study of 3c shows attack has occurred at the α-carbon of the acetylide (with respect to the ruthenium atom) resulting in formation of a σ,π-bound allenyl fragment. Complex 3c crystallizes in the triclinic space group P$\bar{1}$ with cell constants a = 9.626 (1), b = 19.770 (3), c = 21.294 (2) Å, α = 119.18 (1)°, β = 100.28 (1)°, γ = 91.13 (1)°, and Z = 4. With use of 5767 independent reflections ($I \geq 3\sigma(I)$) the structure was solved via the heavy-atom method and refined to R = 0.037 and R_w = 0.045. Solution NMR studies of 3a and 3b reveal rapid interchange of the R groups. A mechanism is proposed whereby exchange of the R groups occurs via a zwitterionic transition state involving rotation about the methylene carbon–sp carbon double bond.

Carbon–carbon bond-forming processes are of fundamental importance in synthesis and catalysis and the study of such reactions at a metal center is a central theme of organometallic chemistry.[1] Attention is now being focussed on the potential of bi- and polynuclear systems to accomplish novel chemical transformations not accessible via mononuclear complex chemistry. Of particular interest in this regard are recent observations[2] of carbon–carbon coupling reactions between unsaturated hydrocarbyl groups coordinated to two or more metals and divalent carbon fragments such as methylene (CH$_2$) or its derivatives either generated from diazoalkane precursors or present as μ-alkylidene ligands. Thus for example Knox and co-workers[2a] reported the synthesis of the vinylcarbene complex (η^5-C$_5$H$_5$)$_2$Ru$_2$(CO)(μ-C(Ph)=CHCH$_3$) via the intermediacy of a μ-methylene complex, from the reaction of the μ-acetylene derivative (η^5-C$_5$H$_5$)$_2$Ru$_2$(CO)(μ-PhC≡CPh) with diazomethane. Two groups, those of Pettit[2b] and Bergman,[2c] described the generation of propylene from the reaction of binuclear μ-methylene complexes Fe$_2$(CO)$_8$(μ-CH$_2$) and (η^5-C$_5$H$_5$)$_2$Co(CO)$_2$(μ-CH$_2$) with ethylene, via the proposed intermediacy of bimetallocyclopentane complexes. A number of other closely related reactions of binuclear μ-methylene complexes have also been reported.[3]

Our own work in this area derived from earlier observations[4] of facile C–C bond-forming reactions between isocyanides and μ_2-η^2- or μ_3-η^2-acetylides to generate mesoionic three-carbon fragments and we recently reported[5] that coupling of diazomethane derived methylene with a μ_3-η^2-acetylide in the trinuclear ruthenium cluster Ru$_3$-(CO)$_6$(μ-CO)$_2$(μ_3-η^2-C≡C-*i*-Pr)(μ-PPh$_2$) occurs rapidly leading to the addition of one and two carbon atoms to the hydrocarbon chain. The facility with which these carbon–carbon bond-forming reactions occurred at ambient temperatures or below contrasts sharply with the vigorous conditions needed to achieve methylene transfer to a coordinated acetylene in the osmium trimer Os$_3$(CO)$_9$(μ-CH$_2$)(μ_3-η^2-PhC≡CPh).[2d,e] We believe that the enhanced reactivity of the multisite bound acetylides in molecules such as 1, particularly toward nucleophiles, can be attributed at least in part to their description as alkylidyne carbides where the "bare" carbidic carbon atom and the alkylidyne, CR fragment are considered as adjacent skeletal atoms in an M$_n$(C)(CR) framework.[6] Such a description suggested that μ_2-η^2-acetylides in the binuclear complexes M$_2$(CO)$_6$(μ_2-η^2-C≡CR)(μ-PPh$_2$) (M = Fe, Ru, Os; 2) should also be reactive since here the alkylidyne–carbide description implies an analogy to an M$_4$ butterfly skeleton. In this paper we describe the reactions of the

(1) (a) Katz, T. J. *Adv. Organomet. Chem.* **1977**, *16*, 283. (b) Grubbs, R. H. *Prog. Inorg. Chem.* **1978**, *24*, 1. (c) Calderon, N.; Lawrence, J. P.; Ofstead, E. A. *Adv. Organomet. Chem.* **1979**, *17*, 449. (d) Ivin, K. J.; Rooney, J. J.; Stewart, C. D.; Green, M. L. H.; Mahtab, R. *J. Chem. Soc., Chem. Commun.* **1978**, 604. (e) Forster, D. *Adv. Organomet. Chem.* **1979**, *17*, 255. (f) Falbe, J. *Carbon Monoxide in Organic Synthesis*; Springer-Verlag: Berlin, 1970. (g) Pruett, R. L. *Adv. Organomet. Chem.* **1979**, *17*, 1. (h) Masters, C. *Homogeneous Transition Metal Catalysis—A Gentle Art*; Chapman and Hall: New York, 1981 and references contained therein. (i) Collman, J. P.; Hegedus, L. S. *Principles and Applications of Organotransition Metal Chemistry*; University Science Books: Mill Valley, CA, 1980.
(2) (a) Colborn, R. E.; Dyke, A. F.; Knox, S. A. R.; MacPherson, K. A.; Orpen, A. G. *J. Organomet. Chem.* **1982**, *239*, C15. (b) Sumner, C. E., Jr.; Collier, J. A.; Pettit, R. *Organometallics* **1982**, *1*, 1350. (c) Theopold, K. H.; Bergman, R. G. *J. Am. Chem. Soc.* **1981**, *103*, 2489. (d) Shapley, J. R.; Sievert, A. C.; Churchill, M. R.; Wasserman, H. J. *J. Am. Chem. Soc.* **1981**, *103*, 6975. (e) Clauss, A. D.; Shapley, J. R.; Wilson, S. R. *J. Am. Chem. Soc.* **1981**, *103*, 7387. (f) Hoel, E. L.; Ansell, G. D.; Leta, S. *Organometallics* **1984**, *3*, 1633.

(3) (a) Dyke, A. F.; Knox, S. A. R.; Naish, P. J.; Taylor, G. E. *J. Chem. Soc., Chem. Commun.* **1980**, 803. (b) Cooke, M.; Davies, D. L.; Guerchais, J. E.; Knox, S. A. R.; Mead, K. A.; Roué, J.; Woodward, P. *Ibid.* **1981**, 862. (c) Herrmann, W. A. *Adv. Organomet. Chem.* **1982**, *20*, 159 and references therein. (d) Isobe, K.; Andrews, D. G.; Mann, B. E.; Maitlis, P. E. *J. Chem. Soc., Chem. Commun.* **1981**, 809. (e) Herrmann, W. A.; Plank, J.; Riedel, D.; Ziegler, M. L.; Weidenhammer, K.; Guggolz, E.; Balbach, B. *J. Am. Chem. Soc.* **1981**, *103*, 63. (f) Hursthouse, M. B.; Jones, R. A.; AbdulMalik, K. M.; Wilkinson, G. *Ibid.* **1979**, *101*, 4128. (g) Hahn, J. E. *Prog. Inorg. Chem.* **1984**, *31*, 205.
(4) MacLaughlin, S. A.; Johnson, J. P.; Taylor, N. J.; Carty, A. J.; Sappa, E. *Organometallics* **1983**, *2*, 352.
(5) Nucciarone, D.; Taylor, N. J.; Carty, A. J. *Organometallics* **1984**, *3*, 177.
(6) (a) Carty, A. J. *Pure Appl. Chem.* **1982**, *54*, 113. (b) Carty, A. J. Alcan Award Lecture, Chemical Institute of Canada, Montreal, 1984. (b) Carty, A. J. Alcan Award Lecture, Chemical Institute of Canada, Montreal, 1984. (c) For a theoretical discussion see: Halet, J. F.; Saillard, J. Y.; Lissillour, R.; McGlinchey, M. J.; Jaouen, G. *Inorg. Chem.* **1985**, *24*, 1695.

carbene precursors diazomethane, dimethyldiazomethane and diphenyldiazomethane with the diruthenium compound **2** (M = Ru; R = Ph) leading to the synthesis via C–C coupling of novel allenyl complexes $Ru_2(CO)_6(\mu_2\text{-}\eta^2\text{-}R_2C\text{=}C\text{=}CPh)(\mu\text{-}PPh_2)$ (**3**). The X-ray structure of **3** (R = Ph) and the fluxional behavior of these unusual molecules are also discussed.

Experimental Section

General Procedures and Instrumentation. All solvents used were dried and distilled under N_2 prior to use. CH_2Cl_2 was dried over phosphorus pentoxide, and heptane was dried over $LiAlH_4$.

Infrared spectra were obtained on a Perkin-Elmer 180 spectrophotometer. Samples for infrared analysis were dissolved in cyclohexane and run in matched NaCl cells of 0.5-mm path length.
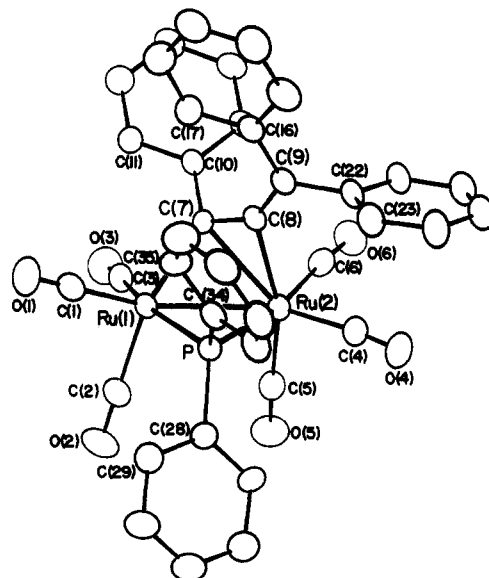
^{13}C NMR spectra were recorded on a Bruker WH-400 spectrometer operating at 100.6 MHz, ^{31}P NMR spectra at 101.2 MHz on a Bruker AM-250 spectrometer, and ^1H NMR spectra at 80 MHz on a Bruker WP-80 instrument. Chemical shifts are referenced to Me_4Si for ^1H and ^{13}C and to 85% H_3PO_4 for ^{31}P. Deuterated toluene was the solvent of choice for both the variable-temperature ^1H and ^{13}C studies while ^{31}P spectra were run in benzene-d_6. Deuterated solvents also provided the lock signal. Samples of **3a** for ^{13}C NMR were enriched by replacing the nitrogen atmosphere in a 50-mL Schlenk tube containing a CH_2Cl_2 (10 mL) solution of **3a** (300 mg) with carbon monoxide gas containing 94.8% ^{13}CO. This solution was left for 3 days, evacuated, refilled with ^{13}CO, and left for an additional 3 days whereupon enriched **3a** was isolated by precipitation from hexane.

Elemental analyses were carried out by Guelph Chemical Laboratories, Ltd., Guelph, Ontario.

Syntheses. $Ru_2(CO)_6(\mu_2\text{-}\eta^2\text{-}H_2C\text{=}C\text{=}CPh)(\mu\text{-}PPh_2)$ (3a). In CH_2Cl_2 (5 mL) was dissolved $Ru_2(CO)_6(\mu_2\text{-}\eta^2\text{-}C\text{≡}CPh)(\mu\text{-}PPh_2)$ (**2**; 200 mg, 0.305 mmol). Freshly prepared diazomethane[7] in ether (ca. 0.2 M) was added at room temperature in 2-mL aliquots until IR analysis of reaction samples indicated complete consumption of starting material. To this solution was added Florisil, and the solvent was stripped off leaving behind a dry, coated powder which was then placed on a dry-packed Florisil column. Elution with heptane removed a yellow band which upon concentration to ~5 mL and refrigeration resulted in precipitation of a pale yellow solid. The isolated yield of **3a** was 141 mg (69%): IR ν(CO) 2075 s, 2044 s, 2011 s, 1995 s, 1980 m cm^{-1}; $^{31}P\{^1H\}$ NMR 138.3 ppm. Anal. Calcd for $Ru_2PO_6C_{27}H_{17}$: C, 48.36; H, 2.56. Found: C, 48.58; H, 2.70.

$Ru_2(CO)_6(\mu_2\text{-}\eta^2\text{-}(CH_3)_2C\text{=}C\text{=}CPh)(\mu\text{-}PPh_2)$ (3b). In CH_2Cl_2 (5 mL) was dissolved **2** (550 mg, 0.839 mmol). To this stirred solution at room temperature was added 3-mL aliquots of an approximately 2 M ether solution of $N_2C(CH_3)_2$ (prepared from acetone hydrazone[8]) every hour for a total of 8 h. Chromatography as for **3a** gave an initial yellow band of starting material (84 mg) followed by product which was also yellow in color. Concentration and crystallization from heptane gave 306 mg (52%) of **3b**: IR ν(CO) 2078 s, 2048 s, 2014 s, 1993 m, 1978 m cm^{-1}; $^{31}P\{^1H\}$ NMR 127.9 ppm. Anal. Calcd for $Ru_2PO_6C_{29}H_{21}$: C, 49.86; H, 3.03. Found: C, 49.65; H, 3.07.

$Ru_2(CO)_6(\mu_2\text{-}\eta^2\text{-}Ph_2C\text{=}C\text{=}CPh)(\mu\text{-}PPh_2)$ (3c). In a Schlenk tube was added **2** (500 mg, 0.762 mmol) and toluene (15 mL). This solution was heated in an oil bath held at 75–80 °C under an atmosphere of carbon monoxide while periodically (every hour) adding ca. 2-mL portions of freshly prepared diphenyldiazomethane (prepared from benzophenone hydrazone[9]) in petroleum ether. Monitoring by infrared showed the reaction to be about half complete after 5 h. At this stage the heat was turned off, ca. 6 mL diphenyldiazomethane solution added, and the mixture left to stir for 18 hours. Column chromatography as for **3a** gave 40 mg of starting material and 223 mg of **3c** (36%): IR ν(CO) 2076 s, 2051 s, 2013 s, 1998 m, 1979 m cm^{-1}; $^{31}P\{^1H\}$ NMR 127.1

(7) DeBoer, T. J.; Backer, H. J. *Org. Synth.* **1956**, *36*, 16.
(8) (a) Andrews, S. D.; Day, A. C.; Raymond, P.; Whiting, M. C. *Org. Synth.* **1970**, *50*, 27. (b) Day, A. C.; Whiting, M. C. *Org. Synth.* **1970**, *50*, 3.
(9) Smith, L. I.; Howard, K. L. *Organic Syntheses*; Wiley: New York, 1955; Coll. Vol. 3, pp 351–352.

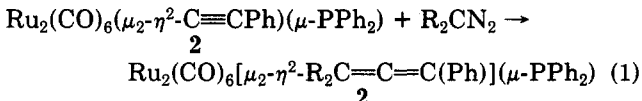**Figure 1.** An Ortep II plot of the structure of molecule A of $Ru_2(CO)_6[\mu_2\text{-}\eta^2\text{-}Ph_2C\text{=}C\text{=}C(Ph)](\mu\text{-}PPh_2)$ (**3c**).

ppm. Anal. Calcd for $Ru_2PO_6C_{39}H_{25}$: C, 56.93; H, 3.06. Found: C, 57.04; H, 3.39.

Crystal Data. Crystals of $Ru_2PO_6C_{39}H_{25}$ (mol wt 822.74) are triclinic of space group $P\bar{1}$ with $a = 9.626$ (1) Å, $b = 19.770$ (3) Å, $c = 21.294$ (2) Å, $\alpha = 119.18$ (1)°, $\beta = 100.28$ (1)°, $\gamma = 91.13$ (1)°, $V = 3454.1$ (7) Å^3 at $T = 293 \pm 1$ K, $Z = 4$, $\rho_{measd} = 1.56$, $\rho_{calcd} = 1.582$ g cm^{-3}, $F(000) = 1640$, and μ(Mo Kα) = 9.49 cm^{-1}.

Collection and Reduction of X-ray Data. Intensity data were collected on a crystal of dimensions 0.24 × 0.25 × 0.31 mm using θ–2θ scans (3.2 < 2θ < 42.0°) with variable scan speeds of 2.93–29.30° min^{-1} and a scan width of 0.75° below Kα_1 to 0.75° above Kα_2 on a Syntex P2$_1$ diffractometer. From a total of 7451 measured reflections, 5767 unique data had $I \geq 3\sigma(I)$ and were used in the structure solution and refinement. Two standard reflections (500; 12,$\bar{1}$,0) monitored after every 100 measurements showed only minor fluctuations. Data were corrected for Lorentz and polarization effects but not absorption. Transmission factors varied between 0.71 and 0.81. The four ruthenium atoms were located in a Patterson synthesis and light atoms via a subsequent Fourier map. Refinement of all non-hydrogen atoms with isotropic thermal parameters gave an R value ($R = \sum||F_o| - |F_c||/\sum|F_o|$) of 0.059. Anisotropic refinement converged at $R = 0.037$ and $R_w = 0.045$ ($R_w = [\sum w(||F_o| - |F_c||^2/\sum||F_o|^2]^{1/2}$; $w^{-1} = 1.89 - 0.0137|F_o| + 0.00017|F_o|^2)$. The thermal parameters were refined in two blocks. Although not included in the refinement, all hydrogen atoms were readily locatable in a final difference Fourier map with electron densities in the range 0.35–0.6 e Å^{-3}. Otherwise, the map was featureless with maximum residuals ~0.45 e Å^{-3} in the vicinity of the ruthenium atoms. Scattering factor tables including anomalous dispersion corrections for ruthenium were taken from ref 10. Programs used are described elsewhere.[11] Atomic positional parameters are listed in Table I. Tables of structure factors and anisotropic thermal parameters are available as supplementary material.

Results and Discussion

Reaction of the diazoalkanes R_2CN_2 (R = H, CH_3, Ph) with the σ–π-acetylide **2** (R = Ph) proceeds as shown in eq 1, affording 36–69% yields of complexes analyzing as $Ru_2(CO)_6(R_2C_3Ph)(PPh_2)$. The new compounds **3a–c**

$$Ru_2(CO)_6(\mu_2\text{-}\eta^2\text{-}C\text{≡}CPh)(\mu\text{-}PPh_2) + R_2CN_2 \rightarrow$$
$$\mathbf{2}$$
$$Ru_2(CO)_6[\mu_2\text{-}\eta^2\text{-}R_2C\text{=}C\text{=}C(Ph)](\mu\text{-}PPh_2) \quad (1)$$
$$\mathbf{2}$$

(10) *International Tables for X-ray Crystallography*; Kynoch Press: Birmingham, England, 1974; Vol. IV.
(11) Carty, A. J.; Mott, G. N.; Taylor, N. J.; Yule, J. E. *J. Am. Chem. Soc.* **1978**, *100*, 3051.

Table I. Fractional Coordinates (×10⁴) for Molecules A and B of $Ru_2(CO)_6[\mu_2\text{-}\eta^2\text{-}Ph_2C\!\!=\!\!C\!\!=\!\!C(Ph)](\mu\text{-}PPh_2)$ (3c)

atom	x	y	z	atom	x	y	z
	A. Molecule A				B. Molecule B		
Ru(1)	−1154.2 (6)	−1355.8 (3)	2651.2 (3)	Ru(1)	2987.8 (6)	932.8 (3)	2535.0 (3)
Ru(2)	781.2 (6)	−2153.3 (3)	1799.2 (3)	Ru(2)	5294.8 (6)	2044.9 (3)	2955.3 (3)
P	−1632 (2)	−2600 (1)	1623 (1)	P	3408 (2)	2182 (1)	3567 (1)
O(1)	−3413 (6)	−1444 (4)	3439 (3)	O(1)	−205 (6)	572 (4)	2173 (4)
O(2)	−3077 (7)	−704 (4)	1815 (4)	O(2)	3553 (7)	256 (3)	3568 (3)
O(3)	269 (7)	339 (3)	3671 (3)	O(3)	3726 (7)	−599 (3)	1317 (3)
O(4)	1232 (6)	−3630 (3)	451 (3)	O(4)	6765 (7)	3684 (3)	4089 (3)
O(5)	82 (7)	−1233 (3)	993 (3)	O(5)	6947 (7)	1215 (3)	3683 (4)
O(6)	3898 (6)	−1412 (3)	2304 (3)	O(6)	7420 (7)	1602 (4)	1937 (4)
C(1)	−2540 (8)	−1392 (4)	3151 (4)	C(1)	994 (9)	696 (4)	2305 (4)
C(2)	−2373 (8)	−947 (4)	2120 (4)	C(2)	3338 (8)	503 (4)	3182 (4)
C(3)	−219 (8)	−290 (4)	3315 (4)	C(3)	3447 (9)	−30 (4)	1742 (5)
C(4)	1113 (8)	−3085 (4)	975 (4)	C(4)	6226 (8)	3080 (5)	3637 (4)
C(5)	316 (8)	−1572 (4)	1296 (4)	C(5)	6311 (9)	1522 (5)	3412 (5)
C(6)	2732 (8)	−1668 (4)	2147 (4)	C(6)	6581 (8)	1751 (4)	2285 (5)
C(7)	583 (7)	−1799 (4)	3014 (3)	C(7)	3308 (7)	1505 (4)	1951 (4)
C(8)	917 (7)	−2545 (4)	2599 (4)	C(8)	3641 (7)	2313 (4)	2296 (4)
C(9)	1286 (7)	−3190 (4)	2620 (4)	C(9)	3274 (8)	2944 (4)	2268 (4)
C(10)	1611 (7)	−1302 (4)	3734 (4)	C(10)	3291 (8)	1072 (4)	1137 (4)
C(11)	1061 (8)	−834 (4)	4356 (4)	C(11)	2204 (10)	439 (4)	673 (4)
C(12)	1977 (9)	−435 (5)	5055 (4)	C(12)	2071 (11)	70 (5)	−100 (5)
C(13)	3428 (9)	−482 (5)	5149 (5)	C(13)	3014 (13)	303 (6)	−400 (5)
C(14)	3965 (8)	−949 (4)	4529 (4)	C(14)	4067 (12)	939 (5)	59 (5)
C(15)	3075 (7)	−1360 (4)	3836 (4)	C(15)	4190 (9)	1324 (5)	832 (4)
C(16)	1052 (8)	−3370 (4)	3188 (4)	C(16)	1871 (8)	2958 (4)	1856 (4)
C(17)	503 (8)	−2854 (5)	3786 (4)	C(17)	825 (8)	2310 (5)	1522 (5)
C(18)	355 (11)	−3010 (6)	4346 (5)	C(18)	−491 (10)	2297 (6)	1109 (6)
C(19)	677 (11)	−3725 (6)	4290 (6)	C(19)	−777 (10)	2970 (7)	1056 (6)
C(20)	1183 (11)	−4243 (6)	3695 (6)	C(20)	247 (11)	3616 (6)	1397 (6)
C(21)	1409 (9)	−4068 (5)	3153 (5)	C(21)	1555 (9)	3615 (5)	1801 (5)
C(22)	1976 (7)	−3762 (4)	2032 (4)	C(22)	4312 (8)	3676 (4)	2674 (4)
C(23)	1261 (8)	−4507 (4)	1502 (4)	C(23)	3960 (10)	4349 (5)	3261 (5)
C(24)	1964 (9)	−5037 (4)	973 (5)	C(24)	4926 (14)	5023 (5)	3656 (6)
C(25)	3329 (8)	−4841 (5)	963 (5)	C(25)	6247 (13)	5032 (6)	3468 (6)
C(26)	4024 (8)	−4098 (5)	1475 (5)	C(26)	6622 (11)	4366 (6)	2885 (5)
C(27)	3352 (8)	−3565 (4)	2015 (4)	C(27)	5613 (9)	3678 (5)	2484 (5)
C(28)	−2946 (7)	−2736 (4)	830 (4)	C(28)	3784 (8)	2291 (4)	4481 (4)
C(29)	−4383 (8)	−2739 (5)	884 (4)	C(29)	2683 (9)	2055 (5)	4711 (5)
C(30)	−5445 (9)	−2842 (6)	284 (5)	C(30)	2889 (11)	2196 (6)	5428 (5)
C(31)	−5069 (9)	−2937 (6)	−345 (4)	C(31)	4178 (11)	2588 (5)	5932 (5)
C(32)	−3662 (9)	−2930 (5)	−402 (5)	C(32)	5248 (10)	2805 (5)	5703 (5)
C(33)	−2579 (8)	−2835 (4)	192 (4)	C(33)	5065 (9)	2657 (5)	4974 (4)
C(34)	−2096 (7)	−3475 (4)	1658 (4)	C(34)	2225 (7)	2935 (4)	3722 (4)
C(35)	−2225 (8)	−3445 (4)	2312 (4)	C(35)	906 (8)	2772 (5)	3260 (5)
C(36)	−2563 (9)	−4134 (5)	2311 (5)	C(36)	−13 (9)	3350 (5)	3406 (5)
C(37)	−2797 (9)	−4857 (5)	1662 (5)	C(37)	398 (9)	4087 (5)	4011 (5)
C(38)	−2680 (8)	−4880 (4)	1010 (5)	C(38)	1712 (11)	4253 (5)	4472 (5)
C(39)	−2317 (8)	−4202 (4)	996 (5)	C(39)	2665 (9)	3679 (4)	4333 (4)

exhibit IR spectra rather similar to that of 2 (R = Ph) with five ν(CO) bands in the terminal region. A single ^{31}P NMR resonance in the range 127–140 ppm, downfield from 85% H_3PO_4, is consistent with retention of the μ-PPh₂ group across the Ru–Ru bond.[12] In order to establish precisely the nature of the hydrocarbyl fragment an X-ray analysis of 3c was carried out. The compound crystallizes in space group $P\bar{1}$ with two independent binuclear molecules in the asymmetric unit. An Ortep plot of one molecule is shown in Figure 1. Selected distances and angles are found in Tables II and III. Since there are only small differences between the two molecules only structural parameters for the A molecules will be discussed here. As expected from the ^{31}P data the basic core of the molecule is similar to that

in 2 (R = t-Bu).[12e] The two ruthenium atoms are held together by a metal–metal bond of length 2.7894 (8) Å (cf. 2.7523 (3) Å in 2 (R = t-Bu)) and a slightly asymmetric phosphido bridge (Ru(1)–P = 2.324 (2) Å, Ru(2)–P = 2.367 (2) Å), with the angle Ru(1)–P–Ru(2) (73.0 (0)°) being typical of μ-PPh₂ groups when a strong metal–metal interaction is present.[13] The hydrocarbon ligand is bonded to the two metal atoms through C(7) and C(8) the carbon atoms of the original alkynyl group. An electron count and an examination of the interatomic distances indicate that the new hydrocarbyl ligand is best considered as a three-electron donor, interacting with Ru(1) via a σ-bond to C(7) and with Ru(2) via an η^2-interaction with C(7)–C(8). The exoskeletal double bond C(8)–C(9) has a bond length of

(12) (a) Ritchey, J. M.; Zozulin, A. J.; Wrobleski, D. A.; Ryan, R. R.; Wasserman, H. J.; Moody, D. C.; Paine, R. T. *J. Am. Chem. Soc.* **1985**, *107*, 501. (b) Roberts, D. A.; Steinmetz, G. R.; Breen, M. J.; Shulman, P. M.; Morrison, E. D.; Duttera, M. R.; DeBrosse, C. W.; Whittle, R. R.; Geoffroy, G. L. *Organometallics* **1983**, *2*, 846. (c) Petersen, J. L.; Stewart, R. P., Jr., *Inorg. Chem.* **1980**, *19*, 186. (d) Carty, A. J.; MacLaughlin, S. A.; Taylor, N. J. *J. Organomet. Chem.* **1981**, *204*, C27. (e) Carty, A. J. *Adv. Chem. Ser.* **1982**, *No. 196*, 163. (f) Garrou, P. *Chem. Rev.* **1981**, *81*, 229. (g) Johannsen, G.; Stelzer, O. *Chem. Ber.* **1977**, *110*, 3438.

(13) See, for example: (a) Field, J. S.; Haines, R. J.; Moore, M. H.; Smit, D. N.; Steer, L. M. *S. Afr. J. Chem.* **1984**, *37*, 138. (b) Rosen, R. P.; Geoffroy, G. L.; Bueno, C.; Churchill, M. R.; Ortega, R. B. *J. Organomet. Chem.* **1983**, *89*, 254. (c) Regragui, R.; Dixneuf, P. H.; Taylor, N. J.; Carty, A. J. *Organometallics* **1984**, *3*, 1020. (d) Patel, V.; Cherkas, A.; Nucciarone, D.; Taylor, N. J.; Carty, A. J. *Organometallics* **1985**, *4*, 1792. (e) MacLaughlin, S. A.; Taylor, N. J.; Carty, A. J. *Organometallics* **1983**, *2*, 1194. (f) *Ibid.* **1984**, *3*, 392. (g) Carty, A. J.; MacLaughlin, S. A.; Taylor, N. J. *J. Chem. Soc., Chem. Commun.* **1981**, 476.

Table II. Bond Distances (Å) in Molecules A and B of Ru$_2$(CO)$_6$[μ$_2$-η^2-Ph$_2$C=C=C(Ph)](μ-PPh$_2$) (3c)

	A	B		A	B
Ru(1)–Ru(2)	2.7894 (8)	2.7832 (8)	Ru(1)–P	2.324 (2)	2.333 (2)
Ru(2)–P	2.367 (2)	2.364 (2)	Ru(1)–C(1)	1.869 (8)	1.884 (8)
Ru(1)–C(2)	1.940 (9)	1.930 (9)	Ru(1)–C(3)	1.954 (8)	1.958 (9)
Ru(2)–C(4)	1.910 (8)	1.914 (9)	Ru(2)–C(5)	1.929 (9)	1.912 (10)
Ru(2)–C(6)	1.932 (8)	1.939 (8)	Ru(1)–C(7)	2.102 (7)	2.101 (8)
Ru(2)–C(7)	2.374 (6)	2.367 (7)	Ru(2)–C(8)	2.173 (7)	2.179 (7)
P–C(28)	1.819 (7)	1.818 (8)	P–C(34)	1.816 (9)	1.829 (8)
C(1)–O(1)	1.155 (10)	1.130 (10)	C(2)–O(2)	1.127 (12)	1.136 (11)
C(3)–O(3)	1.128 (11)	1.123 (11)	C(4)–O(4)	1.139 (10)	1.139 (11)
C(5)–O(5)	1.136 (12)	1.143 (14)	C(6)–O(6)	1.143 (10)	1.139 (11)
C(7)–C(8)	1.382 (11)	1.395 (12)	C(7)–C(10)	1.499 (9)	1.510 (10)
C(8)–C(9)	1.350 (12)	1.329 (12)	C(9)–C(16)	1.469 (11)	1.481 (11)
C(9)–C(22)	1.495 (10)	1.502 (11)			
C(10)–C(11)	1.402 (10)	1.418 (12)	C(11)–C(12)	1.405 (11)	1.417 (12)
C(12)–C(13)	1.387 (11)	1.385 (16)	C(13)–C(14)	1.391 (12)	1.401 (16)
C(14)–C(15)	1.388 (11)	1.417 (12)	C(15)–C(10)	1.402 (10)	1.385 (12)
C(16)–C(17)	1.391 (11)	1.401 (13)	C(17)–C(18)	1.398 (15)	1.399 (13)
C(18)–C(19)	1.404 (19)	1.417 (19)	C(19)–C(20)	1.367 (16)	1.386 (17)
C(20)–C(21)	1.405 (16)	1.393 (15)	C(21)–C(16)	1.398 (14)	1.395 (15)
C(22)–C(23)	1.407 (12)	1.413 (12)	C(23)–C(24)	1.406 (12)	1.388 (16)
C(24)–C(25)	1.369 (12)	1.403 (18)	C(25)–C(26)	1.391 (13)	1.410 (16)
C(26)–C(27)	1.401 (12)	1.430 (15)	C(27)–C(22)	1.385 (10)	1.383 (12)
C(28)–C(29)	1.408 (11)	1.403 (12)	C(29)–C(30)	1.410 (13)	1.386 (13)
C(30)–C(31)	1.375 (13)	1.403 (14)	C(31)–C(32)	1.382 (13)	1.360 (15)
C(32)–C(33)	1.419 (12)	1.409 (12)	C(33)–C(28)	1.388 (10)	1.382 (11)
C(34)–C(35)	1.393 (11)	1.383 (11)	C(35)–C(36)	1.393 (15)	1.407 (14)
C(36)–C(37)	1.398 (14)	1.380 (15)	C(37)–C(38)	1.392 (13)	1.378 (14)
C(38)–C(39)	1.394 (14)	1.424 (14)	C(39)–C(34)	1.415 (11)	1.396 (12)

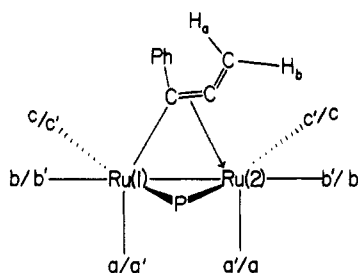**Figure 2.** Structural representation of **3a** showing the labeling scheme used in describing the methylene substituents (H$_a$ and H$_b$) and the carbonyl groups.

1.350 (12) Å typical of the uncoordinated double bond of mononuclear allenes[14] whereas the coordinated bond length C(7)–C(8) (1.382 (11) Å) is significantly longer and falls within the range of values normally observed for η^2-alkene complexes.[15] The three-carbon fragment C(7)–C(8)–C(9) is significantly distorted from linearity with a "bend back" angle at C(8) of 36°. This is an expected and common structural feature of μ$_2$-η^2-acetylide, η^2-allene, and μ$_2$-η^2-allenyl complexes. This value is comparable to those observed for mononuclear, π-only bound, allene ligands of 22–39°.[14,16]
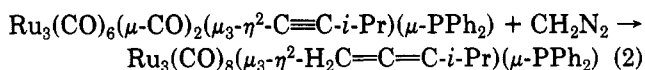
A plane containing Ru(1) and Ru(2) and passing through the midpoint of C(7)–C(8) shows that the allenyl unit is twisted with respect to the metal–metal vector (planes 1A and 1B in Table IV). This twist places C(7) and C(8) on opposite sides of the plane in an effort to maximize the π-interaction of C(7)–C(8) with Ru(2). These deviations from the plane have been calculated as 0.390 Å for both C(7) and C(8) in molecule A and 0.406 Å for both atoms in molecule B. In free allenes the two planes containing the terminal carbon atoms and their substituents are

perpendicular to one another. If Ru(1) is considered to be a substituent on C(7), the corresponding dihedral angle in **3c** between C(7), C(10), Ru(1) (plane 2) and C(9), C(16), C(22) (plane 3) is 65.4° for molecule A and 69.1° for molecule B.

There is an interesting comparison between **3c** and the compound Fe$_2$(CO)$_6$[μ$_2$-η^2-C(CNMe(CH$_2$)$_2$NMe)CPh](μ-PPh$_2$) formed in the reaction of Fe$_2$(CO)$_6$(μ$_2$-η^2-C≡CPh)(PPh$_2$) with the electron-rich olefin [=CN(Me(CH$_2$)$_2$N(Me)]$_2$ which also leads to C–C bond formation. The X-ray structure of this complex revealed a meso-ionic hydrocarbon ligand with a long C$_\alpha$–C$_{carbene}$ bond of length 1.550 (12) Å, distinctly different from the exoskeletal multiple bond seen in **3c**. We will return to this point in connection with the NMR spectra of **3**.

As in the previously reported reaction of a μ$_3$-η^2-acetylide with diazomethane (eq 2), addition of diazoalkanes to **2**

$$Ru_3(CO)_6(\mu\text{-}CO)_2(\mu_3\text{-}\eta^2\text{-}C\equiv C\text{-}i\text{-}Pr)(\mu\text{-}PPh_2) + CH_2N_2 \rightarrow$$
$$Ru_3(CO)_8(\mu_3\text{-}\eta^2\text{-}H_2C=C=C\text{-}i\text{-}Pr)(\mu\text{-}PPh_2) \quad (2)$$

results in coupling of a methylene unit with the α-carbon atom of the acetylide. In both cases the end result is the formation of a μ-η-allenyl group bound as a five-electron ligand in the M$_3$ cluster and a three-electron ligand in the M$_2$ complex.

Several mechanisms can be envisaged for the formation of **3** from **2** and diazoalkanes (Scheme I) including direct attack at the acetylide by "free" alkylidene (Ia), attack by intact diazoalkane at acetylenic carbon (Ib) with subsequent loss of nitrogen, formation of a cyclic pyrazolyl-like intermediate (Ic), and formation of an intermediate carbene complex (Id) with subsequent CR$_2$ transfer onto the acetylide. Mechanism Ia has an analogy in the formation of allenes from acetylenes and gaseous CH$_2$N$_2$ under photolysis,[17] and while we know of no direct exam-

(14) Bowden, F. L.; Giles, R. *Coord. Chem. Rev.* **1976**, *20*, 81.

(15) (a) Mingos, D. M. P. *Adv. Organomet. Chem.* **1977**, *15*, 1. (b) Ittel, S. D.; Ibers, J. A. *Adv. Organomet. Chem.* **1976**, *14*, 33.

(16) (a) Jacobs, T. L. *The Chemistry of Allenes*; Landor, S. R., Ed.; Academic Press: Toronto, 1982; Vol. 2, p 277. (b) Shaw, B. L.; Stringer, A. J. *Inorg. Chim. Acta Rev.* **1973**, *7*, 1.

(17) (a) Rutledge, T. F. *Acetylenes and Allenes*; Reinhold: New York, 1969; Chapter 2. (b) Kirmse, W. *Carbene Chemistry*; Academic Press: New York, 1964, p 34.

Table III. Bond Angles (deg) for Molecules A and B of 3c

	A	B		A	B
		(i) About the Ruthenium Atoms			
Ru(2)-Ru(1)-P	54.2 (0)	54.2 (0)	Ru(2)-Ru(1)-C(1)	147.0 (2)	147.0 (2)
Ru(2)-Ru(1)-C(2)	107.5 (2)	107.0 (2)	Ru(2)-Ru(1)-C(3)	105.8 (2)	105.0 (2)
Ru(2)-Ru(1)-C(7)	56.0 (1)	55.9 (2)	P-Ru(1)-C(1)	101.1 (2)	103.6 (2)
P-Ru(1)-C(2)	90.9 (2)	89.1 (2)	P-Ru(1)-C(3)	158.3 (2)	157.4 (2)
P-Ru(1)-C(7)	84.4 (1)	85.1 (2)	C(1)-Ru(1)-C(2)	92.9 (3)	95.4 (3)
C(1)-Ru(1)-C(3)	100.5 (3)	99.0 (3)	C(1)-Ru(1)-C(7)	105.0 (3)	102.8 (3)
C(2)-Ru(1)-C(3)	87.5 (3)	89.5 (3)	C(2)-Ru(1)-C(7)	162.0 (3)	161.7 (3)
C(3)-Ru(1)-C(7)	90.6 (3)	89.3 (3)	Ru(1)-Ru(2)-P	52.8 (0)	53.1 (0)
Ru(1)-Ru(2)-C(4)	147.0 (2)	147.5 (2)	Ru(1)-Ru(2)-C(5)	86.2 (2)	86.1 (2)
Ru(1)-Ru(2)-C(6)	117.0 (2)	115.4 (2)	Ru(1)-Ru(2)-C(7)	47.2 (1)	47.3 (1)
Ru(1)-Ru(2)-C(8)	75.7 (1)	75.7 (1)	P-Ru(2)-C(4)	94.2 (2)	94.4 (2)
P-Ru(2)-C(5)	93.2 (2)	92.8 (2)	P-Ru(2)-C(6)	168.6 (2)	168.2 (2)
P-Ru(2)-C(7)	77.8 (1)	78.8 (1)	P-Ru(2)-C(8)	78.6 (1)	78.8 (2)
C(4)-Ru(2)-C(5)	97.2 (3)	97.8 (3)	C(4)-Ru(2)-C(6)	95.8 (3)	96.9 (3)
C(4)-Ru(2)-C(7)	134.7 (3)	134.6 (3)	C(4)-Ru(2)-C(8)	99.7 (3)	99.2 (3)
C(5)-Ru(2)-C(6)	90.9 (3)	89.2 (3)	C(5)-Ru(2)-C(7)	127.5 (3)	127.1 (3)
C(5)-Ru(2)-C(8)	161.7 (3)	161.6 (3)	C(6)-Ru(2)-C(7)	91.2 (2)	90.7 (3)
C(6)-Ru(2)-C(8)	94.3 (3)	95.8 (3)	C(7)-Ru(2)-C(8)	35.0 (2)	35.4 (2)
		(ii) About Phosphorus			
Ru(1)-P-Ru(2)	73.0 (0)	72.7 (0)	Ru(1)-P-C(28)	117.1 (2)	119.4 (2)
Ru(1)-P-C(34)	123.6 (2)	124.5 (2)	Ru(2)-P-C(28)	120.9 (2)	119.2 (2)
Ru(2)-P-C(34)	120.3 (2)	122.8 (2)	C(28)-P-C(34)	101.8 (3)	99.1 (3)
		(iii) About the Carbonyl Carbon Atoms			
Ru(1)-C(1)-O(1)	177.3 (3)	178.3 (3)	Ru(1)-C(2)-O(2)	179.5 (3)	179.3 (3)
Ru(1)-C(3)-O(3)	175.8 (3)	175.8 (3)	Ru(2)-C(4)-O(4)	174.8 (3)	174.3 (3)
Ru(2)-C(5)-O(5)	177.9 (3)	178.5 (4)	Ru(2)-C(6)-O(6)	175.3 (3)	174.7 (3)
		(iv) About the Allenyl Carbon Atoms			
Ru(1)-C(7)-Ru(2)	76.8 (1)	76.8 (1)	Ru(1)-C(7)-C(8)	123.4 (2)	122.4 (3)
Ru(1)-C(7)-C(10)	121.7 (2)	122.8 (3)	Ru(2)-C(7)-C(8)	64.5 (2)	64.9 (3)
Ru(2)-C(7)-C(10)	130.0 (2)	128.5 (3)	C(10)-C(7)-C(8)	114.8 (4)	114.7 (4)
Ru(2)-C(8)-C(7)	80.5 (2)	79.7 (3)	Ru(2)-C(8)-C(9)	135.3 (3)	136.9 (3)
C(7)-C(8)-C(9)	144.0 (4)	143.4 (4)	C(8)-C(9)-C(16)	124.1 (4)	122.6 (4)
C(8)-C(9)-C(22)	118.7 (4)	119.0 (4)	C(16)-C(9)-C(22)	117.3 (4)	118.4 (4)
		(v) About the Phenyl Ring Carbons			
C(7)-C(10)-C(11)	118.2 (4)	117.5 (4)	C(7)-C(10)-C(15)	123.1 (4)	122.3 (4)
C(15)-C(10)-C(11)	118.2 (4)	119.9 (5)	C(10)-C(11)-C(12)	119.8 (4)	118.9 (5)
C(11)-C(12)-C(13)	121.6 (5)	120.8 (6)	C(12)-C(13)-C(14)	118.2 (5)	120.1 (6)
C(13)-C(14)-C(15)	121.0 (5)	119.5 (6)	C(14)-C(15)-C(10)	121.1 (4)	120.7 (5)
C(9)-C(16)-C(17)	122.0 (4)	120.3 (4)	C(9)-C(16)-C(21)	120.5 (4)	121.0 (5)
C(21)-C(16)-C(17)	117.5 (5)	118.6 (5)	C(16)-C(17)-C(18)	121.7 (5)	121.6 (5)
C(17)-C(18)-C(19)	120.1 (6)	118.4 (6)	C(18)-C(19)-C(20)	118.5 (6)	120.1 (6)
C(19)-C(20)-C(21)	121.5 (6)	120.5 (6)	C(20)-C(21)-C(16)	120.7 (5)	120.7 (6)
C(9)-C(22)-C(23)	121.0 (4)	119.3 (4)	C(9)-C(22)-C(27)	119.7 (4)	119.8 (4)
C(27)-C(22)-C(23)	119.3 (4)	120.8 (5)	C(22)-C(23)-C(24)	119.2 (4)	119.9 (6)
C(23)-C(24)-C(25)	121.3 (5)	119.8 (6)	C(24)-C(25)-C(26)	119.5 (5)	121.2 (6)
C(25)-C(26)-C(27)	120.2 (5)	118.3 (6)	C(26)-C(27)-C(22)	120.5 (4)	120.0 (5)
P-C(28)-C(29)	117.2 (3)	118.2 (3)	P-C(28)-C(33)	122.6 (3)	122.2 (3)
C(33)-C(28)-C(29)	120.2 (5)	119.3 (5)	C(28)-C(29)-C(30)	119.5 (5)	119.8 (5)
C(29)-C(30)-C(31)	119.8 (5)	120.7 (5)	C(30)-C(31)-C(32)	121.3 (5)	119.3 (6)
C(31)-C(32)-C(33)	119.8 (5)	120.8 (5)	C(32)-C(33)-C(28)	119.4 (4)	120.1 (5)
P-C(34)-C(35)	121.9 (3)	121.2 (3)	P-C(34)-C(39)	118.2 (3)	118.4 (3)
C(39)-C(34)-C(35)	119.9 (4)	120.3 (5)	C(34)-C(35)-C(36)	119.7 (5)	120.4 (5)
C(35)-C(36)-C(37)	121.2 (5)	120.2 (5)	C(36)-C(37)-C(38)	118.7 (5)	119.7 (5)
C(37)-C(38)-C(39)	121.3 (5)	121.2 (5)	C(38)-C(39)-C(34)	119.1 (4)	118.2 (5)

ples of organic intermediates analogous to Ib, transition-metal complexes of intact CR_2N_2 are known.[18] Cyclic intermediates of the type shown in Ic are attractive since $μ_2$-$η^2$-acetylides are known to undergo both $α$- and $β$-attack depending on the nucleophile and pyrazoles are products from the reaction of diazomethane with acetylenes in ether solution.[17] Although the generation of an intermediate carbene complex by displacement of the $π$-bound acetylide as in Id is potentially feasible, there is no evidence for analogous adducts in the reactions of 2 with phosphines, amines, or isocyanides by low-temperature NMR spec-

(18) (a) Herrmann, W. A.; Schweizer, I. *Z. Naturforsch., B*; 1978, *33B*, 911. (b) Chisholm, M. H.; Folting, K.; Huffman, J. C.; Raterman, A. L. *Inorg. Chem.* 1984, *23*, 2303. (c) Nakamura, A.; Yoshida, T.; Cowie, M.; Otsuka, S.; Ibers, J. A. *J. Am. Chem. Soc.* 1977, *99*, 2108. (d) Ferguson, G.; Laws, W. J.; Parvez, M.; Puddephatt, R. *J. Organometallics* 1983, *2*, 276. (e) Herrmann, W. A.; Kriechbaum, G.; Ziegler, M. L.; Wulknitz, P. *Chem. Ber.* 1981, *114*, 276.

Table IV. Equations of Planes for 3c: A and B Refer to the Unique Molecules in the Unit Cell[a]

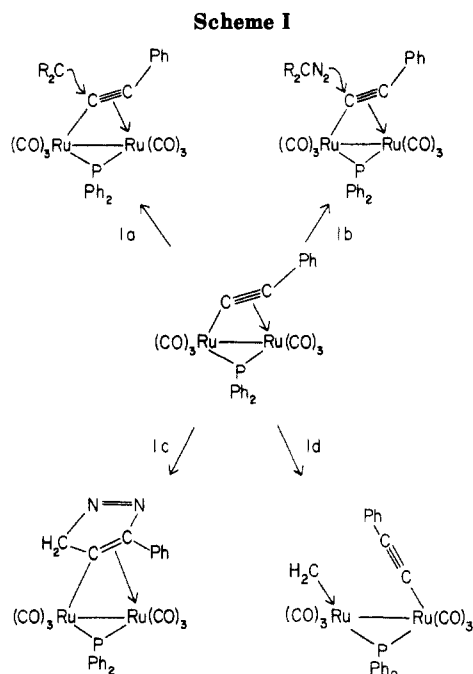| plane	equation
1A	$0.55936X + 0.65039Y + 0.51392Z + 2.22825 = 0$
1B	$-0.59469X + 0.37334Y + 0.71201Z - 1.85953 = 0$
2A	$0.66861X + 0.58518Y - 0.45884Z + 6.78047 = 0$
2B	$0.96632X - 0.15781Y + -0.20330Z - 2.87625 = 0$
3A	$0.79313X - 0.24345Y + 0.55828Z - 0.74448 = 0$
3B	$-0.56262X - 0.13836Y + 0.81506Z - 1.65529 = 0$

[a] Atoms defining the planes are found in the text.

troscopy.[22] Further mechanistic data will be necessary to firmly establish which of mechanisms Ia–d is operative in the formation of 3.

We earlier made reference to the description of $μ$-$η$-bound acetylides in polynuclear complexes as alkylidyne carbides. Reference to the structure for the M_2-acetylide complexes emphasizes the "open" nature of the unsub-

Scheme I

stituted α-carbon atom (the "carbido" carbon) in these molecules. There is now a great deal of chemical evidence to suggest that carbon atoms in these acetylides are electrophilic, behaving in terms of reactivity rather like Fischer-type carbenes.[19] Thus the acetylide ligand has been shown to be susceptible to nucleophilic attack at both the α- and β-positions depending on the nature of the acetylide substituent and the nucleophile. Thus, reaction with phosphites,[20] isocyanides,[21] and amines[11,22] results in carbon–phosphorus, carbon–carbon, and carbon–nitrogen bond formation, respectively. With soft carbon donors such as isocyanides and now carbenes attack has only been observed at C_α.

Comparison of the reactivity of the μ_3-η^2- vs. μ_2-η^2-bonded acetylide shows that reaction of the former is qualitatively much more rapid than the latter. Reaction of $Ru_3(CO)_6(\mu\text{-}CO)_2(\mu_3\text{-}\eta^2\text{-}C\equiv C\text{-}i\text{-}Pr)(\mu\text{-}PPh_2)$ is essentially complete upon addition of diazomethane whereas with 2 the reaction is sluggish and requires copious amounts of diazomethane added at room temperature over a period of several hours in order to achieve complete conversion. Although such differences might simplistically be attributed to greater ligand activation in the M_3 cluster where the acetylide interacts with three metals, it may well be that different mechanisms are operative in the two cases. This viewpoint is supported by the observation that no reaction occurs between $(\mu\text{-}H)Ru_3(CO)_9(\mu_3\text{-}\eta^2\text{-}C\equiv C\text{-}t\text{-}Bu)$ or $Os_3(CO)_9(\mu_3\text{-}\eta^2\text{-}C\equiv C\text{-}i\text{-}Pr)(PPh_2)$ with diazomethane under similar conditions. In contrast the rapid reaction of $Ru_3(CO)_6(\mu\text{-}CO)_2(\mu_3\text{-}\eta^2\text{-}C\equiv C\text{-}i\text{-}Pr)(\mu\text{-}PPh_2)$ with Lewis bases (CO, phosphines) leads us to believe that the reaction depicted in eq 2 proceeds via precoordination of diazomethane to a metal site. Lacking a detailed knowledge of the mechanism of the formation of 3, it would be inappropriate to directly compare the reactivity of the acetylide ligand in M_2 and M_3 systems.

(19) Dötz, K. H.; Fischer, H.; Hofmann, P.; Kreissl, F. R.; Schubert, U.; Weiss, K. *Transition Metal Carbene Complexes*; Verlag-Chemie: Deerfield Beach, FL, 1983.

(20) (a) Wong, Y. S.; Paik, H. N.; Chieh, P. C.; Carty, A. J. *J. Chem. Soc., Chem. Commun.* 1975, 309. (b) Carty, A. J.; Taylor, N. J.; Paik, H. N.; Smith, W. F.; Yule, J. *Ibid.* 1976, 41.

(21) Carty, A. J.; Mott, G. N.; Taylor, N. J. *J. Organomet. Chem.* 1981, 212, C54.

(22) Mott, G. N.; Carty, A. J. *Inorg. Chem.* 1983, 22, 2726.
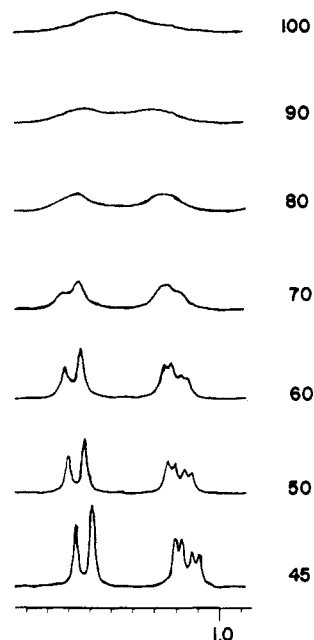
Figure 3. Variable-temperature ¹H NMR spectra of 3a. Small divisions represent 0.1 ppm increments. The temperature (°C) at which each spectrum was taken is found to the right of each respective spectrum.

Fluxional Behavior of $Ru_2(CO)_6\text{-}(\mu_2\text{-}\eta^2\text{-}R_2C\text{=}C\text{=}CPh)(\mu\text{-}PPh_2)$. The observation of a puzzling room-temperature ¹H NMR spectrum for 3a led to variable-temperature NMR studies of 3a and 3b. Derivative 3c contains only phenyl protons, and NMR spectra provide little information that cannot be gleaned from 3a and 3b.

The ¹H NMR spectrum of 3a at 30 °C is representative of the low-temperature slow-exchange limit. The methylene protons of 3a are diastereotopic and give rise to signals centered at 1.64 and 1.16 ppm (Figure 3). The low-field signal is an AB doublet with J_{AB} = 6.2 Hz, and the high-field signal is an ABX doublet of doublets with J_{AB} = 6.2 Hz and J_{HX} = 2.4 Hz. The larger J value is assigned to coupling between the diastereoptic protons while the smaller value is assigned to coupling of hydrogen to phosphorus. The latter represent four bonding couplings. We assign the ABX doublet of doublets at 1.16 ppm to H_a and the AB doublet at 1.64 ppm to H_b on the following basis. Referring to Figure 1, if C(16) and C(22) are replaced by H_a and H_b, respectively, we note that H_a adopts a trans stereochemistry relative to the η^2-interaction of the allenyl fragment with Ru(2) while H_b is cis to this η^2-interaction. A well-known rule in determining the stereochemistry about double bonds is that trans couplings are invariably larger than cis. Although in this case Ru(2) is the substituent trans to H_a rather than phosphorus, with the latter being attached to Ru(2), we feel that $J_{H_a\text{-}P}$ should be larger than $J_{H_b\text{-}P}$. As the temperature increases, the peaks broaden and coalesce (Figure 3). At the highest temperature attained (100 °C) the fast-exchange limiting spectrum had still not been achieved. Indeed a value of 100 °C appears to be a reasonable estimate of the coalescence temperature.

Before discussing a possible mechanism for site exchange of the diastereotopic protons of 3a, it is appropriate to discuss the ¹H NMR spectra of 3b. Apart from phenyl protons which give rise to signals in the 6.7–7.8 ppm range the only other features of the low-temperature limiting spectrum of 3b are a pair of doublets arising from the diastereotopic methyl groups. The low field signal at 1.28 ppm has $J_{H\text{-}P}$ = 3 Hz while the doublet at 1.07 ppm has $J_{H\text{-}P}$ = 4 Hz. Arguments used in assigning the methylene
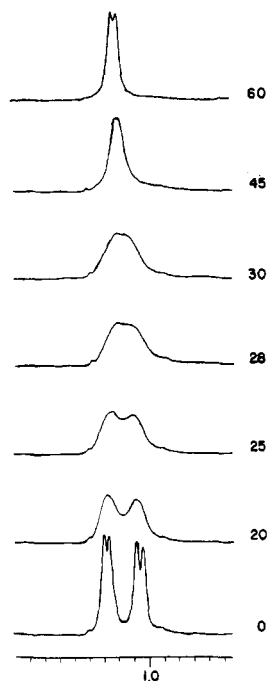
Figure 4. Variable-temperature ^{1}H NMR spectra of **3b**. The temperature (°C) is found to the right of each spectrum, and divisions are in 0.1 ppm increments.

Table V. ^{13}C NMR Data Associated with the Slow-Exchange Limiting Spectrum of **3a**

CO	δ	J_{PC}, Hz
a	198.42	<1
b	197.71	9
c	196.32	72
a′	196.98	<1
b′	199.53	12
c′	195.76	62

protons of **3a** should be applicable here; hence the slightly larger J_{HP} value for the high-field doublet is used tentatively to assign this signal to the methyl group Me_a "trans" to Ru(2). Likewise the low-field doublet with the smaller J_{H-P} value is assigned to the "cis" methyl group Me_b. In contrast to the variable-temperature spectra of **3a**, **3b** shows a lower coalescence temperature of 30 °C and the fast-exchange limit is attainable in toluene-d_8 with the observation of a doublet at 60 °C. The spectral changes observed in the methyl region are shown in Figure 4 for selected temperatures.

The ^{13}C spectra of ^{13}CO-enriched **3a** were obtained at different temperatures. The carbonyl region is shown in Figure 5. The static structure is frozen out at 20 °C. An examination of the solid-state structure of **3c** (Figure 1) reveals that none of the carbonyls are symmetry-related; thus six unique resonances are expected and found. Interpretation of the ^{13}C carbonyl region is simplified somewhat since the six carbonyls can be divided into three unique pairs with respect to their disposition relative to the equatorial phosphorus atom. Thus carbonyls a/a′ adopt a cis axial configuration while c/c′ have a trans stereochemistry and b/b′ carbonyls are cis equatorial, intermediate between a/a′ and c/c′ with respect to phosphorus. The magnitudes of the carbon–phosphorus couplings are expected to increase in the order

$$J_{P-C_{aa'}} < J_{P-C_{bb'}} < J_{P-C_{cc'}}$$

Thus a partial assignment can be made as found in Table V and illustrated in Figure 2. Raising the temperature results in broadening and collapse of *three* of the six carbonyl resonances (Figure 5). Each of the three carbo-
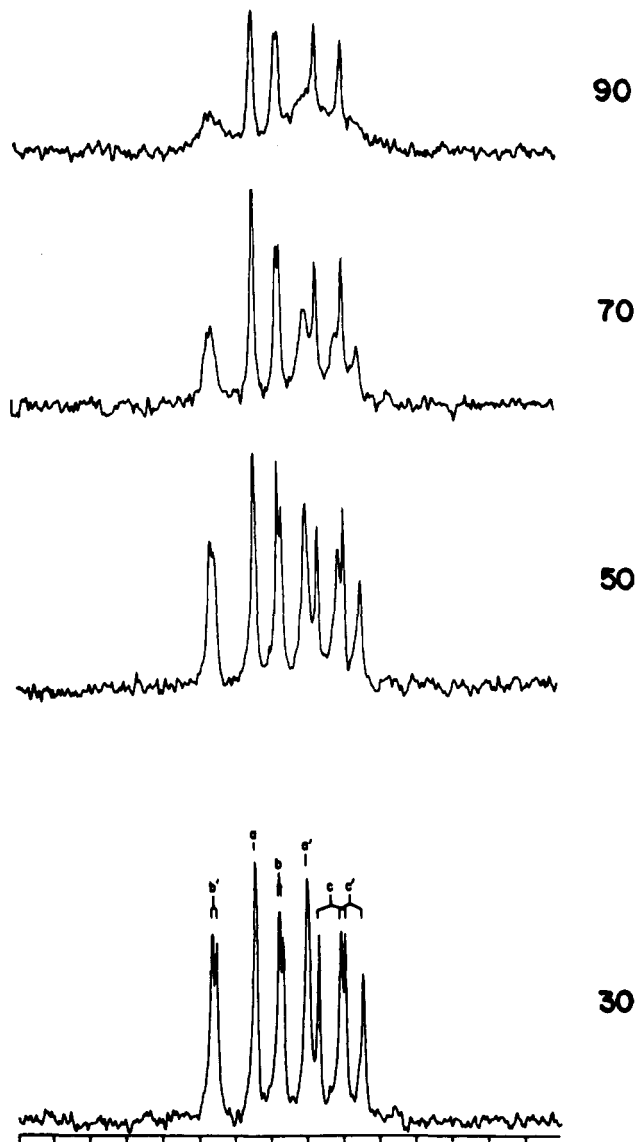

Figure 5. Variable-temperature ^{13}C NMR spectra of **3a** showing the region from 190 to 205 ppm. Divisions are in 1 ppm increments.

nyls involved in the exchange occupies a unique position relative to the phosphorus atom; i.e., the exchanging set of carbonyls is made up of one each of type a, b, and c carbonyls. For reasons to be seen later these three carbonyls are assigned to one ruthenium atom while the other three "static" carbonyls are assigned to the other metal atom. We do not have enough information to allow unequivocal assignment of the sets (a, b, c) and (a′, b′, c′) to either Ru(1) or Ru(2).

Mechanism of Fluxionality of $Ru_2(CO)_6(\mu_2$-η^2-R_2C=C=$CPh)(\mu$-$PPh_2)$. Fluxional behavior in mononuclear π-allenes has been well documented and described.[23] Three distinct processes have been observed: (i) rotation about the metal–π bond as frequently seen in metal–olefin complexes; (ii) an orthogonal 1,2 shift of the metal atom; (iii) syn–anti isomerization of the allene resulting from consecutive, orthogonal 1,2 shifts. The possibility that similar mechanisms may be invoked to describe the fluxionality in our system is not likely in view

(23) (a) Ben-Shoshan, R.; Pettit, R. *J. Am. Chem. Soc.* **1967**, *89*, 2231. (b) Vrieze, K.; Volger, H. C.; Praat, A. P. *J. Organomet. Chem.* **1970**, *21*, 467. (c) Hewitt, T. G.; DeBoer, J. J. *J. Chem. Soc.* **1971**, 817. (d) Foxman, B.; Marten, B.; Rosan, A.; Raghu, S.; Rosenblum, M. *J. Am. Chem. Soc.* **1977**, *99*, 2160. (e) Vrieze, K.; van Leeuwen, P. W. N. M. *Prog. Inorg. Chem.* **1971**, *14*, 1.
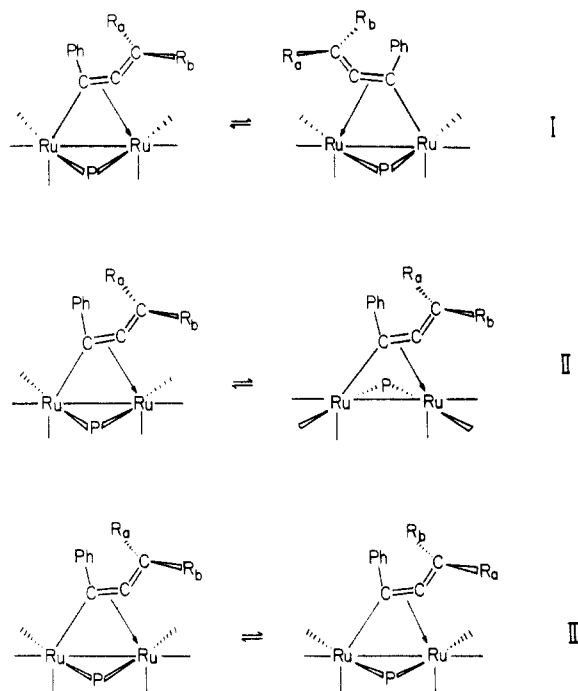
Figure 6. Possible ways of interchanging the methylene R groups. Phenyl groups on phosphorus are omitted.

of the fact that the allenyl ligand is anchored to the dimer through a metal–carbon σ bond. This difference in bonding between π- and σ–π-allenes eliminates (i) (although a variant will be discussed) while (ii), even if physically possible, could not exchange R_a and R_b, and it follows then that since (ii) is not possible, neither is (iii).

A mechanism that accounts for the site exchange of the methylene protons in **3a** and the methyl groups in **3b** must also account for the observation of only one signal in the ^{31}P NMR spectra of **3a–c**. The first mechanism is depicted in Figure 6. This mechanism (labeled mechanism I) involves a flipping back and forth of the allenyl fragment such that the σ- and π-bonding interactions to the metal atoms are reversed. Such a process has been described independently by Shapley and co-workers for σ–π-vinyl-type ligands bound to hydridoosmium clusters[24] and by Brown et al. for rhenium dimers.[25] A similar exchange is believed to occur in bimetallic rhenium acetylides[26] as well as in phosphido-bridged iron, ruthenium, and osmium acetylides.[27] Such a mechanism is consistent with both the ^{1}H and ^{31}P NMR of **3a–b** data but cannot be reconciled with the ^{13}C spectra. If such a mechanism was operative, the ^{13}CO NMR spectra should show broadening and merging of each pair of signals constituting the sets aa', bb', and cc', resulting in a fast-exchange limiting spectrum consisting of three resonances. Simple calculations show that coalescence of peaks c and c' should occur at 105 °C.[28] Clearly the ^{13}C data suggest that such a process is not

occurring. What is observed is a broadening and collapse of only carbonyls a', b', and c' while the set a, b, and c remain relatively unaffected. Such an observation is consistent with the presence of a second dynamic process, turnstile rotation of three carbonyl groups bound to one of the ruthenium atoms. The relationship of this second dynamic process to the first, if any, is not clear at the present time, but the ^{13}C studies serve to eliminate mechanism I as an explanation for the exchange of R_a and R_b.

A second mechanism is depicted by II in Figure 6. Here we consider the possibility of oscillation of the phosphido bridge from one side of the dimer to the other accompanied by a slight twist of the allenyl fragment. Fluxional behavior in phosphido bridges, as well as in germanido bridges, has been observed.[29] Such a process would in this case be consistent with both the ^{1}H and ^{31}P NMR results but not with the ^{13}C data.

Evidence against II was obtained by an examination of the temperature dependence of the ^{13}C resonances arising from the carbons of the phosphido bridge phenyl rings. At room temperature rapid rotation about the P–C_{ipso} bond results in site exchange of the ortho and separately the meta carbons. Consequently, since the phenyl rings are chemically nonequivalent, two resonances are expected for the ortho carbons as well as two for the meta carbons. The ipso and para carbons will give rise to a single resonance for each ring. These C_{ipso} and C_{ortho} resonances generally fall in the region of 130–140 ppm and are conveniently removed from the clutter of other aromatic resonances found upfield. As such, at room temperature, **3a** shows doublets for the ipso carbons at 140.15 (J_{PC} = 2.92 Hz) and 133.05 (J_{PC} = 25.5 Hz) ppm and two doublets for the ortho carbons at 133.5 (J_{PC} = 10.1 Hz) and 133.16 (J_{PC} = 10.7 Hz) ppm. The exchange process described by II can be differentiated from III (vide infra) in that the former will show site exchange of the ipso and ortho carbons while the latter will not. With a separation $\Delta\nu$ = 24 Hz, a coalescence temperature of 93 °C is obtained for the ortho carbon resonances of **3a** (using $\Delta G^{\ddagger}$ = 18.7 kcal mol^{-1}). When run in toluene-d_8 at 90 °C, the ortho carbon signals remained sharp and distinct with no sign of broadening. These results clearly eliminate II.

The interchange of hydrogen atoms in μ,η^2-vinyl ligands has been reported.[30-32] In particular Deeming and co-workers demonstrated that pyridine-catalyzed isomerization about the C–C double bond in $(\mu$-H)Os$_3(\mu_2$-η^2-CH= CH$_2$)(CO)$_{10}$ occurred by nucleophilic attack at the β-carbon atom to give a zwitterionic alkylidene intermediate.[30] The generation of such an alkylidene intermediate in the present context may be envisaged as occurring via nucleophilic attack by water, present as solvent impurity, at C(8). The methylene substituents could then interchange by rotation about the C(7)–C(8) bond. While Deeming was

(24) (a) Shapley, J. R.; Richter, S. I.; Tachikawa, M.; Keister, J. B. *J. Organomet. Chem.* **1975**, *94*, C43. (b) Clauss, A. D.; Tachikawa, M.; Shapley, J. R.; Pierpont, C. G. *Inorg. Chem.* **1981**, *20*, 1528.

(25) Nubel, P. O.; Brown, T. L. *J. Am. Chem. Soc.* **1984**, *106*, 644.

(26) (a) Nubel, P. O.; Brown, T. L. *Organometallics* **1984**, *3*, 29. (b) Lee, K.-W.; Pennington, W. T.; Wallace Cordes, A.; Brown, T. L. *J. Am. Chem. Soc.* **1985**, *107*, 631.

(27) (a) Carty, A. J.; MacLaughlin, S. A.; Cherkas, A., to be submitted for publication. (b) Koridze, A. A.; Kizas, O. A.; Kolobova, N. E.; Petrovskii, P. V. *Bull. Acad. Sci. USSR, Div. Chem. Sci.* **1984**, 437.

(28) At a field strength of 100 MHz $\Delta\nu$(c–c') = 56.3 Hz. This gives a rate k = 125 s^{-1} from k = $\pi\Delta\nu/(2)^{1/2}$. Using $\Delta G^{\ddagger}$ = 18.7 kcal mol^{-1} (obtained from the ^{1}H NMR results) in the approximate equation k = (k_BT/h) exp($-\Delta G^{\ddagger}/RT$) gives T = 105 °C as the coalescence temperature. These calculations are not meant to be a substitute for a complete and more accurate line-shape analysis, yet provide a first approximation.

(29) (a) Harley, D. A.; Whittle, R. R.; Geoffroy, G. L. *Organometallics* **1983**, *2*, 383. (b) Burdett, J. K. *J. Chem. Soc., Dalton Trans.* **1977**, 423. (c) Coleman, J. M.; Dahl, L. F. *J. Am. Chem. Soc.* **1967**, *89*, 542. (d) Ginsburg, R. E.; Rothrock, R. E.; Finke, R. G.; Collman, J. P.; Dahl, L. F. *J. Am. Chem. Soc.* **1979**, *101*, 6550. (e) Adams, R. D.; Cotton, F. A.; Cullen, W. R.; Hunter, D. L.; Mihichuk, L. *Inorg. Chem.* **1975**, *14*, 1395. (f) Flood, T. C.; DiSanti, F. J.; Campbell, K. D. *Inorg. Chem.* **1978**, *17*, 1643. (g) Dessy, R. E.; Rheingold, A. L.; Howard, G. D. *J. Am. Chem. Soc.* **1972**, *94*, 746. (h) Crowte, R. J.; Evans, J. *J. Chem. Soc., Chem. Commun.* **1984**, 1332. (i) Adams, R. D.; Cotton, F. A. *J. Am. Chem. Soc.* **1970**, *92*, 5003.

(30) Liu, J.; Boyar, E.; Deeming, A. J.; Donovan-Mtunzi, S. *J. Chem. Soc., Chem. Commun.* **1984**, 1182.

(31) Gerlach, R. F.; Duffy, D. N.; Curtis, M. D. *Organometallics* **1983**, *2*, 1172.

(32) Beck, J. A.; Knox, S. A. R.; Riding, G. H.; Taylor, G. E.; Winter, M. J. *J. Organomet. Chem.* **1980**, *202*, C49.
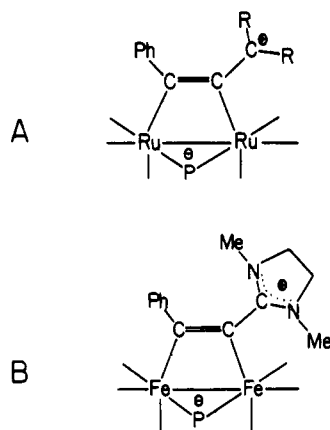
Figure 7. Possible zwitterionic transition state involved in the exchange mechanism (A) and the structure of $Fe_2(CO)_6[\mu_2\text{-}\eta^2\text{-}C(CNMe(CH_2)_2NMe)CPh](\mu\text{-}PPh_2)$ (B).

able to show that the rate of isomerization was dependent on pyridine concentration, addition of excess pyridine to toluene-d_8 solutions of **3a** had no effect on the line shape of the ^1H NMR spectrum at 30 °C, indicating no rate increase. This is interpreted as indicating that the generation of a similar μ-alkylidene intermediate is not responsible for the fluxional behavior of **3a**.

A third possibility (mechanism III) involves an interchange of R groups on the allenyl group by rotation about the exoskeletal bond C(8)–C(9). This exchange process, which is consistent with the ^1H and ^{31}P data and not inconsistent with the ^{13}C spectra, can be envisaged as occurring via a zwitterionic transition state in which C(8)–C(9) is a single bond, C(9) is carbocationic, and the negative end of the dipole, formally on C(7) (or C(8)), is delocalized into the $Ru_2P(CO)_6$ skeleton (Figure 6).

Evidence in support of mechanism III is that the activation energy for R = CH_3 is lower than for R = H. Using the relationships $k = \pi \Delta \nu / (2)^{1/2}$ and $k = (k_b T/h) \exp(-\Delta G^*/RT)$ values of $\Delta G^* = 18.7$ and 15.6 kcal mol^{-1} for **3a** and **3b**, respectively are obtained. The latter values are calculated for coalescence temperatures of 30 ± 1 °C for **3b** and a value of 100 ± 3 °C for **3a**. This order is entirely consistent with the ability of methyl groups to enhance the

stabilization of carbocations relative to hydrogen substituents.

The most compelling evidence for mechanism III is found in the isolation and characterization of $Fe_2(CO)_6$-$[\mu_2\text{-}\eta^2\text{-}C(CNMe(CH_2)_2NMe)CPh](\mu\text{-}PPh_2)$ depicted in Figure 7B. The X-ray structure of this compound can essentially be considered a snapshot of the proposed transition state. The primary structural features of the latter have already been described,[33] but important points relevant to this discussion need a brief mention here. The C(9)–N bonds are short with an average length of 1.319 (20) Å indicative of multiple-bond character. This is further illustrated by planar stereochemistry about each nitrogen atom. The C(8)–C(9) bond is clearly devoid of multiple-bond character as shown by a bond length of 1.550 (12) Å, while the C(7)–C(8) interaction results in a bond length of 1.21 (3) Å, justifying the presence of strong multiple bonding. The Fe(1)–C(7) and Fe(2)–C(8) bond lengths are essentially identical with values of 2.09 (3) and 2.08 (2) Å, respectively. The angles about the nitrogens N(1) and N(2) are 358.99 and 359.99° clearly showing their planar environment. Taken as a whole, these results point to a delocalized positive charge distributed over the two nitrogen atoms with the negative charge delocalized in the iron core. Such a representation presumably allows free rotation about the C(8)–C(9) bond and thus nicely represents a model to explain the exchange of R groups in **3**.

(33) Carty, A. J.; Taylor, N. J.; Smith, W. F.; Lappert, M. F.; Pye, P. L. *J. Chem. Soc., Chem. Commun.* **1978**, 1017.

Site Selectivity in the Reaction of (η^2-1,3-Cyclohexadiene)Fe(CO)$_3$$^{-\cdot}$ with Hydrogen and Deuterium Atoms

Richard N. McDonald* and A. Kasem Chowdhury

Department of Chemistry, Kansas State University, Manhattan, Kansas 66506

Received November 4, 1985

Thermal energy electrons attach to $(\eta^4\text{-}1,3\text{-}c\text{-}C_6H_8)Fe(CO)_3$ generating $(\eta^2\text{-}1,3\text{-}c\text{-}C_6H_8)Fe(CO)_3^-\cdot$ (1). Reaction of **1** with H atoms gave the fragmentation product ions $(OC)_3FeH^-$, $(OC)_3Fe^-\cdot$, and $(C_6H_8)Fe$-$(CO)_2(H)^-$ in the ratio of 75/20/5. When **1** was allowed to react with D atoms, the major fragment ion product was observed to be composed of $(OC)_3FeD^-$ (69%) and $(OC)_3FeH^-$ (31%). These results are interpreted in terms of principal formation of the Fe–H(D) bond as the primary process with some intramolecular rearrangement (H/D exchange) occurring prior to unimolecular fragmentation of the excited adduct negative ions.

The reactions of organometallic complexes with reactive atomic species (e.g. H, D, N, O) is an area limited to gas-phase investigations. Interest in such reactions extends from (a) their use to generate new, unique structures for

further study to (b) their application in structure characterization of the original complex. The latter application would be especially useful in gas-phase studies of ionic complexes where mass and isotopic analysis is the principal